

# Hydrofaction™ of forestry residues to drop-in renewable transportation fuels

10

*C.U. Jensen\**, *J.K.R. Guerrero†*, *S. Karatzos†*, *G. Olofsson\**, *S.B. Iversen\**

\*Steeper Energy ApS, Hørsholm, Denmark, †Steeper Energy Canada Ltd, S.W. Calgary, AB, Canada

## 10.1 Introduction

On a global and unprecedented scale, climate change is threatening humanity through changing weather patterns and rising sea levels. An increasing frequency of catastrophic droughts and floodings affects essential food and water supply, forcing so-called climate migrants to move due to sudden or gradual changes in the natural environment [1,2]. The Paris agreement (in force November 2016, signed by 193 countries) addresses the urgent and potentially irreversible threat of climate change and the necessity to reduce greenhouse gas (GHG) emissions from the energy sector [2,3]. In the World Energy Outlook 2016 [3], IEA projects the future energy sector and how existing technologies for renewable heat and power generation will be deployed to approach emission targets. This includes a significant increase in electricity generation from, for example, solar and wind, which indirectly introduces renewables in the transportation sector, where electric cars are considered momentous for urban and short-distance transport [3]. However, the same report emphasises that the lack of renewable fuel alternatives for heavy transportation such as trucks and aviation will account for the continued growth in global consumption of fossil and carbon-intensive petroleum [3]. The European Commission also highlights the need for low-emission fuels for heavy transportation in order to meet the emission targets for the transportation sector, which currently represents about 25% of EU's total GHG emissions [4]. Steeper Energy is addressing this gap by commercializing its proprietary hydrothermal liquefaction (HTL) technology, Hydrofaction™, which facilitates the production of sustainable drop-in biofuels targeting heavy transportation.

The competitive strengths of HTL begin from the ability to process a wide range of wet and dry low-value nonfood biomass residues, thereby mitigating feedstock supply risks and interference with food supply. Secondly, HTL is currently considered a competitive and resource-effective thermochemical pathway to advanced biofuels, due to its high energy and carbon efficiency [5,6]. A 2014 study commissioned by the US DoE estimated a 70% GHG emission reduction from hydrotreated HTL biofuel compared with the 2005 petroleum baseline [5]. Finally, the hydrotreated HTL products are fully compatible with the existing petroleum infrastructure (pipelines, stations, and

engines) enabling drop-in without blend-wall limitations. This facilitates a gradual phase-in where production capacity and cost-efficiency can be balanced during the transition to fossil independence [7].

### 10.1.1 *Forestry residues as feedstock*

Steeper Energy is currently focused on forestry residues and mill wastes as Hydrofaction™ feedstock due to the global abundance of these resources and the industry's need for cost- and carbon-efficient utilisation of their wastes.

Forests cover around one-third (30.7% in 2010) [8] of the global land area and are an essential part of life. The significant amounts of carbon that is sequestered both below- and aboveground by photosynthesis also make forests essential for climate-change adaptation and mitigation [8]. As an example, afforestation and reforestation were approved as GHG mitigating strategy under the Kyoto Protocol [9]. Carbon sequestration can be optimised by agroforestry and sustainable forest management, thus enhancing the rate of carbon absorption [8–11]. In other words, since a tree grows slower as it gets older, there is an optimum between the harvest rotation cycle and the rate of carbon uptake. In fact, [11] states that the shorter the harvest rotation age, the more favourable the carbon balance becomes over time. This however implies that the sequestered carbon (wood) is used to substitute fuel-intensive building materials such as steel or concrete, while the manufacturing residues (bark, branches, and sawdust) are used to substitute fossil fuels [11]. Such efficient use of the forestry residues is however not granted, as the industry currently wastes up to 40% of the harvested material [12].

The revenue from residuals is also crucial for the forest industry. This was concluded in a recent study on the biomass supply and utilisation chain in three Canadian provinces [13]. The study showed how sawmills were running at a small loss on their core process, the lumber output, but stayed in business due to revenue from residuals as inputs to, for example, electricity generation. Similarly, if the price of lumber would decrease, only the sawmills located close to residual offtakers (e.g. pulp mill) would stay in operation from the value of the residual products [13]. These residuals (wood chips, sawdust, planer shavings, and residual bark) are mainly produced at the mill during the primary processing. However, the major fraction of forestry residuals is the so-called slash, produced during the preliminary processing at the felling site. These have been estimated to account for more than 20% of the total harvested volume in Canada [12].

As mentioned previously, the forestry residuals need to be used as bioenergy to replace fossil fuels in order for agroforestry to be a carbon-efficient GHG mitigation strategy [11]. As such, the slash can be chipped and transported at a cost around US\$ 30–60/ODT (oven-dried tonne) [12–14]. Due to the costs of processing and transportation, a significant amount of such slash is either disposed in stockpiles or burnt on site instead of being efficiently utilised. Wood waste stockpiles decompose over time releasing significant methane emissions from anaerobic digestion, which has a significant GHG footprint ( $1 \text{ kg CH}_4 = 25 \text{ kg CO}_2\text{e}$ ) [15–17]. A portion of the forest residuals are currently used for electricity and heat types of bioenergy [3,13]. However, in the

longer run, this is unlikely to be a cost-competitive solution to alternative renewable sources such as solar PV and wind power, as IEA projects an average cost reduction on these by 2040 of 40%–70% and 10%–25%, respectively [3]. Furthermore, the pulp industry, which is a major offtaker of forestry residuals, is currently struggling in Europe and North America with a decreasing demand and increasing competition from Asian and South American mills [18,19]. This emphasises the need for finding alternative uses of forestry residuals, such as a feedstock for thermochemical production of bio-fuels. In fact, the transformation of pulp and paper mills into biorefineries in Europe and North America has been mentioned as a potential cornerstone of a green economy [20]. This is where the Hydrofaction™ technology becomes relevant by bridging the gap between a globally abundant waste product that needs to be cost-effectively and carbon effectively utilised and the heavy transportation sector that needs a renewable fuel alternative. A life-cycle GHG emission analysis of Hydrofaction™ products produced in Alberta, Canada, from forestry residuals (slash) as feedstock is presented later in Section 10.3.

## 10.2 The Hydrofaction™ process

Hydrofaction™ is a proprietary thermochemical technology platform that enables conversion of wet (as harvested) biomass residues directly to renewable drop-in bio-fuel indistinguishable from its petroleum equivalent. The reaction pathway includes two major subprocesses, which are supercritical HTL (first stage) and subsequent upgrading through hydrotreating (second stage). During the first stage, Hydrofaction™ utilises a combination of the following features to efficiently convert the biomass to an energy-dense renewable crude oil [21]:

- Operating pressures (300–350 bar) and temperatures (390–420°C) above the critical point of water
- Recirculation of water-soluble organics and Hydrofaction™ oil for improvements in feed characteristics, energy balance, oil quality, and yields
- Use of homogeneous alkali metal catalyst ( $K_2CO_3$  and NaOH) for desired catalytic effects and control of pH to minimise corrosion
- Recovery and recycling of alkali metal catalysts for improved process economics and reduced footprint

The resulting biocrude is characterised by relatively high aromaticity and an oxygen content around 10 wt%, which strongly affects the physiochemical properties (density, viscosity, volatility, polarity, and hydrophobicity) that determine the biocrude compatibility with petroleum equivalents. Therefore, as any petroleum crude, the renewable crude oil needs further refining to meet the various fuel specifications. Whereas hydrodesulphurisation (HDS) and hydrodenitrogenation (HDN) are the major reaction steps in refining petroleum crudes, upgrading of wood-derived HTL crude oil is mostly focused on hydrodeoxygenation (HDO) and hydrodearomatization (HDA). During Hydrofaction™, this is achieved by hydrotreating on commercial catalysts, which is a standard and widely used refinery operation [22]. Finally, the

hydrotreated product is fractionated by boiling point to renewable fuels for drop-in in the diesel and marine fuel pools. Thereby, forestry residues can be used to substitute fossil transportation fuels with a renewable alternative.

The Hydrofaction™ subprocesses are schematised in Fig. 10.1 including major interconnected operations, such as recirculation streams, water treatment, and utilisation of gaseous products in a fired heater. Fig. 10.1 is divided into an HTL and an upgrading part; accordingly, the description and presentation of experimental data for the first and second stage are divided into Sections 10.2.1 and 10.2.2, respectively.

### 10.2.1 Supercritical HTL (first stage)

Characteristics of Hydrofaction™ HTL are the use of high-density, supercritical water; homogenous alkali metal catalysts; and the recycling of aqueous and oil products back into the process. The Hydrofaction™ HTL stage applies operating conditions (300–350 bar and 390–420°C) that are above the critical point of water, which is higher than most other HTL processes reported in literature [23–28]. The chemical properties, such as the dielectric constant and ionic product, that make near-critical water an appealing reaction medium for HTL are a direct function of density [29]. Thus, by ensuring a high pressure, key thermodynamic properties of water can be maintained at the same order of magnitude as for the subcritical conditions while taking advantage of improved kinetics, mass, and heat transfer at higher temperatures. As an example, the ionic product of water is an important parameter within hydrothermal processing, because it reflects whether a medium favours ionic or radical reactions [30,31]. Due to the relatively high

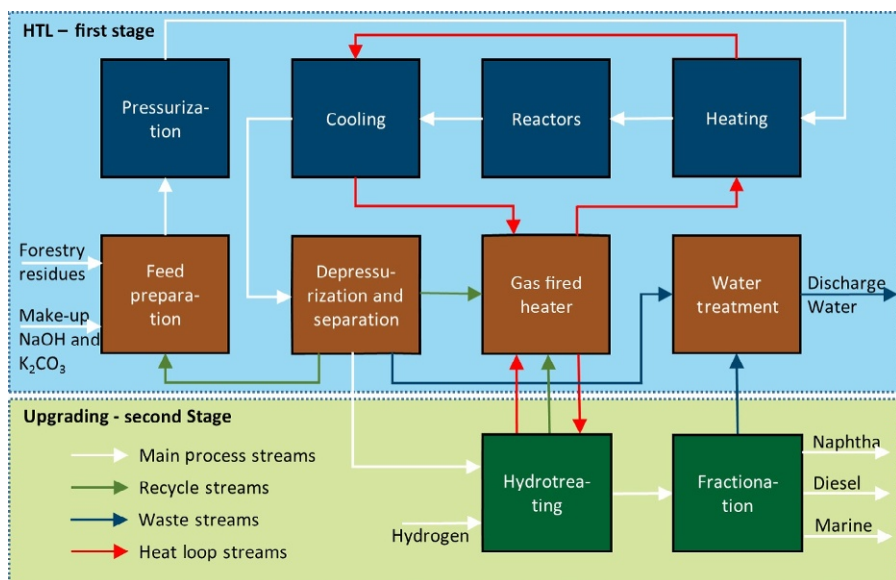


**Fig. 10.1** Schematic of the Hydrofaction™ process consisting of supercritical HTL and subsequent hydrotreating. Besides the major heat loop streams indicated, the process utilises additional heat integration between the stages.

pressure, the ionic product of water at Hydrofaction™ conditions is up to several orders of magnitude higher than at the critical point. Similarly, the higher pressure ensures that density and derived properties are less dependent on temperature changes, which is beneficial during plant operations to ensure a smooth transition of process parameters such as fluid velocities, Reynolds numbers, specific heat capacity, heat-transfer coefficients, and retention times. Consequently, due to the supercritical temperature, it is crucial to maintain a high pressure during the Hydrofaction™ HTL stage.

At near-critical conditions, the dielectric constant of water is reduced more than 90% as compared with ambient conditions. Thereby, water dissolves nonpolar compounds, such as biomass and biocrude molecules that are hydrophobic at ambient conditions. This accelerates conversion through, for example, hydrolysis and solvolysis reactions by reducing mass-transfer limitations. Such ionic reactions are further promoted by water dissociation, which is maintained high in relatively high-density supercritical water [29].

The recirculation of produced organic compounds in the form of both water-soluble organics and oil has a number of benefits. It simplifies feed preparation and reduces the heat capacity of the process fluid, and it appears that the presence of water-soluble organics in the feed inhibits further formation of water-soluble organics, thereby increasing the relative amount of oil produced. Ref. [21] provides further details on the characteristics of Hydrofaction™ HTL, the reasoning behind the operating conditions, and the considerations around the major chemical reactions occurring during the HTL stage.

### 10.2.1.1 Feed preparation

The first step of the HTL stage in Fig. 10.1 is to prepare a pumpable feed of the different reactants including the forestry residues. The feed is prepared from size-reduced forestry residues, recycled oil, and aqueous products as well as make-up homogenous catalysts in the form of potassium carbonate and sodium hydroxide. Recirculation of both the aqueous and oil products is beneficial during feed preparation, because the water-soluble organics and phenolic oil compounds introduce a partial dissolution mechanism, which increases homogeneity and improves rheological properties of the feed. Similarly, the presence of alkali salts gives rise to carbonate/bicarbonate, which accelerates the depolymerisation by hydrolysis during pretreatment. The homogeneous catalyst in the form of potassium is mainly introduced by recirculation of the aqueous products, but make-up is required because a small fraction of the aqueous products are discharged to prevent build-up of trace compounds. Sodium hydroxide is added for control of the pH to alkaline conditions throughout the process.

A high biomass dry-matter loading in the feed is important to drive down both capital and operational expenses per fuel volume produced. Wood feeds with a dry-matter content of 17–25 wt% are used during pilot testing of Hydrofaction™ HTL [21,32,33].

### 10.2.1.2 Pressurization and heating

The feed mixture is pressurised to a pressure in the range of 300–350 bar and subsequently rapidly heated to a reaction temperature in the range of 390–420°C. The heating is to a large degree performed by heat recovered from the outgoing product stream.

This is performed by indirect heat exchange using high-pressure water as heat-transfer medium in a loop from the cooling section to the heating section.

It should be noted that several benefits are provided by the supercritical operating pressure and temperature applied in the Hydrofaction™ process. This is related to the fact that Hydrofaction™, despite being supercritical, is operating below the so-called pseudocritical line (PCL), which is defined as the temperature at a given pressure where the specific heat capacity of water is at a maximum [29]. This means, for example, that the enthalpy of water at, for example, 335 bar and 400°C is similar to the specific enthalpy at the critical point of water [29]. The specific enthalpy of the actual mixture is even lower as water typically only comprises around 50 wt% of the feed mixture due to the high dry-matter and organic content. Recirculation of organics through both the aqueous and oil product reduces the overall heat-transfer requirement, due to the lower specific heat capacity of organics compared with water. This reduces the overall heat requirement of the process, which is emphasised with Fig. 10.2 that shows how the power consumption of the two serially connected heaters in the pilot plant decrease once the process fluid is switched from water to feed at a constant mass flowrate. Note that the pilot does not facilitate heat exchange and thus it has a slightly different configuration than that given for the first stage in Fig. 10.1. The pilot plant is described in Section 10.2.1.6.

Heat exchange is an obvious feature that improves the cost and energy efficiency of a hydrothermal process that utilises near-critical water as a reaction medium. The relatively high pressure applied in Hydrofaction™ ensures that the heat-transfer coefficient of water does not drop above the critical point. Likewise, the higher temperature, compared with subcritical, results in a high thermal effusivity and a more favourable driving force for

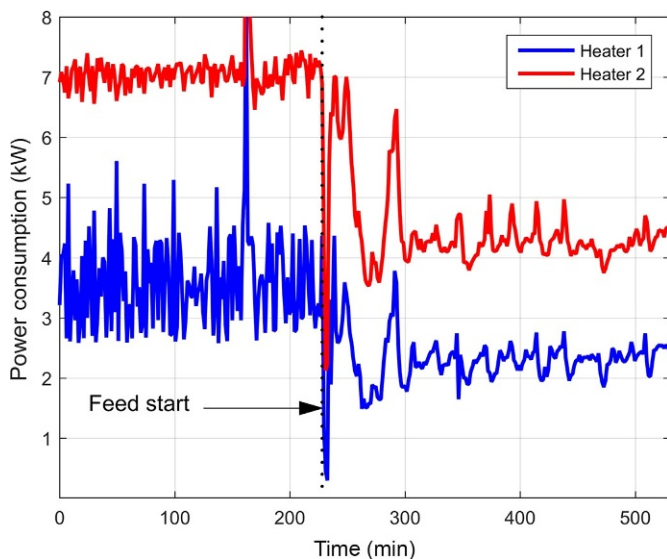


**Fig. 10.2** The effect of switching from water to feed on power consumption of the pilot plant heaters.

heat exchange, which improves the heat recovery potential. Typically, 50%–75% of the heat required for heating to reactor temperature is recovered through heat exchange. The remaining heat load of the process is supplied by a fired heater, which at steady state is fired with gas from the process. This stream possesses more than sufficient calorific value, even if the hydrogen fraction is extracted (for upgrading use) before combustion. In fact, this makes the Hydrofaction™ process self-sustained with thermal energy at steady state.

### 10.2.1.3 Reactors

The heated feed/product intermediate enters the reactors, where it is maintained at reaction temperature and pressure for a certain period of time, typically 10–15 min. A proposed set of major chemical reactions occurring during Hydrofaction™ is presented in Ref. [21].

### 10.2.1.4 Cooling and pressure reduction

The product mixture from the reactors is cooled to about 150°C by heat exchange with the incoming feed via the high-pressure water loop described above, before the pressure is reduced to separation pressure in the pressure let-down system.

### 10.2.1.5 Separation and water treatment

In the separation part of the process, the cooled and depressurised products are separated into a gas stream, a water stream containing dissolved salts, a crude oil stream, and optionally a solid stream. This is performed by a combination of filtration and gravimetric phase separation.

The gas phase produced is mixed with product gas from the upgrading section and used to fuel the fired heater and heat the high-pressure water loop as described above. Optionally, the first-stage gas phase may be further separated to extract hydrogen and/or CO<sub>2</sub> before combustion (see Section 10.3 for details).

The aqueous phase is split into a concentrate and a distillate phase in a recovery unit. The distillate is purified to allow disposal and discharged in amounts that balances the water deducted from the feedstock biomass. The concentrate, which contains most of the total organic carbon (TOC) and alkali metal catalysts, is recycled back to the feed preparation step, except a bleed of 5%–15% that is withdrawn to prevent build-up of trace compounds such as chloride. A fraction of the oil phase is also recycled back to the feed preparation step, while the remainder is conditioned through desalting to recover potassium and sodium alkali catalysts and reduce the ash and water content prior to hydrotreating. The first-stage product is a renewable crude oil that similar to fossil equivalents requires further upgrading to meet transportation fuel specifications.

### 10.2.1.6 Summary of HTL pilot operation data (first stage)

A continuous pilot facility dedicated to supercritical HTL was commissioned at Aalborg University, Denmark, in 1Q2013. Since then, the pilot has completed >1600 oil production hours and constituted a centrepiece in the generation of data from the first stage (HTL) of Hydrofaction™.

The pilot is a semicontinuous HTL plant; feeds are prepared in 100 kg batches and then processed continuously at a flowrate around 20 kg/h. In standby mode between batches, the plant circulates pressurised deionised water, which is also the medium used for heat-up and cool-down of the plant. The batchwise processing of feeds complicates the recirculation of aqueous and oil products, that is, characteristic to Hydrofaction™ HTL. The recirculation is however demonstrated in the pilot by using a start-up oil and recycling the products a number of times until the start-up oil is sufficiently diluted/converted and a steady-state product is produced. Using this approach, it has been observed that recirculation of the aqueous product enhances oil yield, because the TOC content of the aqueous product is stable at steady state [21,33].

Table 10.1 lists key figures on the operating conditions, the feed characteristics, and the product yields observed during an extensive oil production campaign that is published in Ref. [21]. A 50:50 mix of spruce and pine wood chips was used as Hydrofaction™ feedstock to produce >150 kg of renewable Hydrofaction™ crude oil. The total mass balance at steady state was on average 100.3 wt%, with no detectable production of char or filter retentate products. The yield of renewable Hydrofaction™ crude oil from dry ash-free woody biomass was on average 45.3 wt%, and similarly, the gas yield was 41.2 wt%. Based on closure of the carbon, hydrogen, and oxygen elemental balances, the remaining product mass was suggested to be water synthetically produced during the biomass conversion.

### 10.2.1.7 Effect of feedstock on renewable crude oil quality (first stage)

Table 10.2 lists basic physiochemical properties, and Fig. 10.3 depicts distillation profiles of six different renewable Hydrofaction™ crude oils that were produced from three different woody biomass types and using two different start-up oils, crude tall oil (CTO) and distilled tall oil (DTO). The results indicate that the different Hydrofaction™ oils appear to have very similar key characteristics, which emphasises that the start-up oil has little effect on the final product quality because it seems to be diluted sufficiently after 4–6 recirculation cycles. It needs mentioning that the IBP-130°C volatiles were lost during the production of oil A, which increased the viscosity relative to the other oils. The H/C ratio of oil A and the volatility in Fig. 10.3 are also slightly affected by this.

The effect of hardwood (birch) versus softwood (pine/spruce) was also tested at the pilot at the same operating conditions as those given in Table 10.1, but Table 10.2 and Fig. 10.3 indicate only little noticeable difference between the key quality characteristics of the Hydrofaction™ oil produced from the two different types of woody biomass. Though it seems that birch wood results in a slightly higher nitrogen content compared with pine/spruce mixtures. A 10% bark in a pine/spruce feedstock was also tested, based on the motivations previously mentioned for using forestry residues in which bark will be a significant constituent. Again, the quality of the resulting crude oil is comparable, and thus, it could be suggested that a renewable Hydrofaction™ crude oil produced from woody biomass is expected to be relatively viscous; contains roughly 10 wt% oxygen, 1000–2000 ppm nitrogen, and 100–200 ppm sulphur; and possesses an HHV around 38 MJ/kg and a H/C ratio around 1.3–1.4.



**Table 10.1 Key figures on the first-stage Hydrofaction™ HTL are based on Ref. [21]**

Feed characteristics			Operating conditions				Yield figures		
Feedstock		50:50 Spruce/pine	Feed flowrate	kg/h	20–22	Mass balance	wt%	100.3	
Dry-matter content	wt%	17–20	Reactor temperature	C	390–410	Oil yield	wt%	45.3	
Oil-to-wood ratio	kg/kg	0.8–1.0	Reactor pressure	bar	300–320	Gas yield	wt%	41.2	
Particle size	mm	<2	Heating rate	C/min	<350–450	Water yield	wt%	13.8	

**Table 10.2 Basic properties of renewable crude oils produced by Hydrofaction™ of various woody biomasses using different start-up oils**

Oil	Cycle	Start-up oil	Feedstock	Viscosity <sup>a</sup> (cP)	HHV <sup>b</sup> (MJ/kg)	MCR <sup>b,c</sup> (wt%)	C <sup>b</sup> (wt%)	H <sup>b</sup> (wt%)	N <sup>b</sup> (ppm)	S <sup>b</sup> (ppm)	O <sup>d</sup> (wt%)	H/C
Oil A [21]	6	CTO	Pine/spruce	17,360	38.6	21.0	81.4	8.6	1124	100	9.8	1.26
Oil B	4	CTO	Pine/spruce	714	38.0	16.4	80.4	9.0	822	195	10.4	1.34
Oil C	5	CTO	Birch	813	38.0	15.6	80.8	9.1	2635	215	9.8	1.34
Oil D	5	DTO	Birch	2084	37.7	18.6	80.2	9.2	2201	159	10.4	1.37
Oil E	5	DTO	Pine/spruce	3313	37.2	19.7	80.0	9.0	1447	104	10.9	1.34
Oil F	5	DTO	10% Bark in pine/spruce	1954	37.9	18.1	81.4	9.7	973	100	8.8	1.42

<sup>a</sup> Viscosity at 40°C.

<sup>b</sup> On dry basis.

<sup>c</sup> Micro carbon residue (ASTM D4530).

<sup>d</sup> Oxygen by difference.

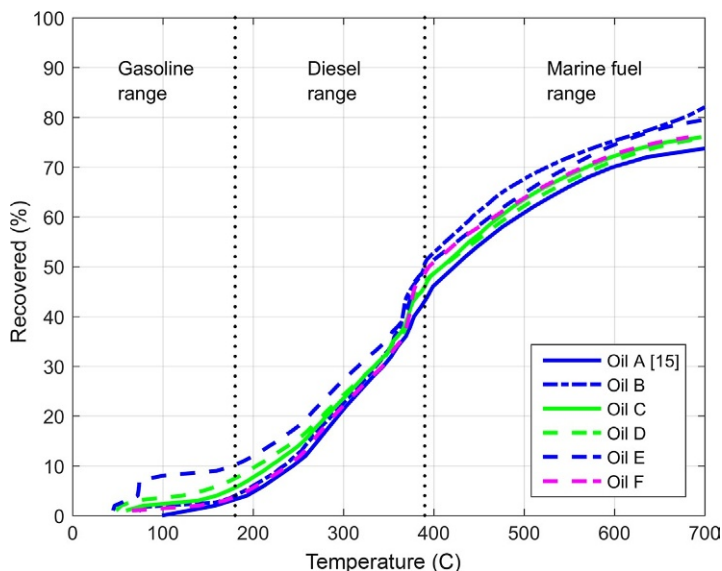


**Fig. 10.3** Simulated distillation (ASTM D7169) of the oils given in Table 10.2 produced from pine/spruce (blue), birch (green), and 10% bark in pine/spruce (purple).

### 10.2.2 Upgrading to drop-in biofuels (second stage)

A significant degree of biomass deoxygenation takes place during the first-stage Hydrofaction™ HTL, but the remaining oxygen content of the renewable crude oil affects the physiochemical properties that determine its compatibility with petroleum equivalents. In other words and similar to petroleum crude oils, the renewable crude oil can be referred to as an intermediate that requires further upgrading in order to gain transportation fuel value. Upgrading of the renewable Hydrofaction™ crude oil is done through catalytic hydrotreatment, which is a widely used process within conventional petroleum refining [22]. The process applies heterogeneous bimetallic catalysts and relatively high partial  $H_2$  pressures to remove oxygen as mainly water through HDO and hydrogenate the renewable crude oil to remove aromatics and improve the diesel and marine fuel characteristics such as cetane number, density, and aromaticity. As indicated with a recirculation stream in Fig. 10.1, the hydrogen produced in situ during the HTL stage can be separated from the gaseous HTL product and utilised to cover part (~50%) of the hydrogen consumption in the second stage.

The current chapter presents hydrotreating experiments carried out in both continuous and batch reactor systems (BRS) and using both sulphided and nonsulphided catalysts. The objective is to show the product quality of wood-derived renewable oil after upgrading while also addressing catalyst activation and stability issues. Catalyst stability is crucial for the economic feasibility of hydrotreating; in petroleum refining, fixed-bed hydrotreating catalysts are generally in operation for several months or years before being regenerated or replaced. Most petroleum hydrotreaters apply sulphided bimetallic catalysts to remove sulphur and nitrogen in, for example,

a middle-distillate fraction. Such sulphided catalysts stay active from the sulphur that is indigenous to the petroleum-derived feed. Hydrofaction™ renewable crude oil contains only 100–200 ppm sulphur, and as shown in the experimental results below, this affects the activity of a sulphided NiMo/Al<sub>2</sub>O<sub>3</sub> catalyst. Based on these observations, two additional approaches were tested in the current study to improve catalyst activity:

- (1) The renewable crude oil was spiked with butanethiol to a total sulphur content of 1 wt% S and upgraded in a continuous fixed-bed reactor system to test if a higher sulphur concentration improved the catalyst activity.
- (2) Alternatively, the use of nonsulphided hydrotreating catalysts was tested as a potential upgrading path that reduces/eliminates the need of expensive gas cleaning operations downstream of the hydrotreater.

The two approaches have been tested experimentally, and the results are presented in the following.

### 10.2.2.1 *Experimental procedure, Hydrotreating studies (second stage)*

Feedstocks for the upgrading experiments presented below were different samples of renewable Hydrofaction™ crude oils produced at the pilot described in [Section 10.2.1.6](#). The oils originate from oil production campaigns similar to that presented in Ref. [21].

### 10.2.2.2 *Continuous reactor system*

The CRS consists of a dual-piston syringe pump that ensures constant volumetric flowrate of oil. The pistons were kept at 90°C to reduce the viscosity and ensure a constant density, which was used to estimate the mass flowrate of oil. Oil and hydrogen were mixed in-line, and pressurised hydrogen was fed at a rate corresponding to 900 NL/L oil in all experiments. The fixed-bed reactor was made of ¾ in. stainless steel tubing, was operated in upflow mode, and was heated by electric heat cables. A 1/8 in. multi-point thermocouple facilitated 10 measurements inside the reactor. The feed mixture was heated at the entrance of the reactor, and the entrance region ensured a constant temperature of the mixture when reaching the catalyst bed. Reactor products were separated at 60°C and operating pressure in a cylindrical vessel. Gases were either collected for compositional analysis or passed through a wet test meter for volumetric flowrate. A back-pressure regulator at the gas-line outlet was used to set the operating pressure of the system.

The experimental results below present two different upgrading campaigns where the CRS was used. Both campaigns used a NiMo/Al<sub>2</sub>CO<sub>3</sub> catalyst (activated in situ by sulphidation), but in the so-called spiked campaign, the renewable crude oil was spiked with butanethiol to increase the total sulphur content to 1 wt% S. The nonspiked campaign was carried out over 16 days (380 h), while the spiked campaign was running for 28 days (660 h) and mass balances were taken at least two times daily.

### 10.2.2.3 Batch reactor system

The BRS consisted of two 25 mL microbatch reactors build from 316L Swagelok fittings that enable pressure logging. The reactors were loaded with reactants, leak tested, and pressurised with H<sub>2</sub> prior to a rapid heat-up by introducing them into a preheated Techne SBL-2D fluidised sand bath with temperature control. Thorough mixing of the reactants was ensured by shaking the reactors at 450 Hz using a shaking device. All experiments were carried out in repeats to ensure accurate data. Gaseous products were quantified by weighing the mass loss during depressurisation into a gas sampling vessel for compositional analysis. Catalysts were filtered off the reactor liquid products, and the latter were centrifuged at 3800 g for 10 min to separate the aqueous and upgraded oil products. Additional details on the BRS upgrading methodology is given in Ref. [34].

Space velocity is a thought parameter in relation to microbatch reactors, but it is advantageous to adapt to the terminology of continuous systems to enable comparison with the CRS experiments. With that in mind, a WHSV equivalent (WHSV\*) incorporating reaction time, oil, and catalyst loading for the BRS experiments was defined as  $\text{WHSV}^* = m_{\text{oil}} / (m_{\text{catalyst}} \times t_{\text{reaction}})$ . The hydrogen availability at initiation of the experiments was 525 NL/L oil.

### 10.2.2.4 Sulphided catalysts

A commercial NiMo/Al<sub>2</sub>O<sub>3</sub> catalyst in the form of 3.2 mm extrudates was used for the sulphided catalyst tests. For the CRS, this catalyst was activated in situ using vacuum gas oil with 3.7 wt% dimethyl disulphide at a liquid hourly space velocity (LHSV) of 1.5 h<sup>-1</sup> and a pressure of 41 bar.

### 10.2.2.5 Nonsulphided catalysts

The nonsulphided catalysts have up until now only been screened in the BRS to evaluate the degree of deoxygenation and hydrogenation that these catalysts can provide. Two different catalyst types were tested, a NiW/SiO<sub>2</sub>/Al<sub>2</sub>O<sub>3</sub> catalyst and a Pd/Al<sub>2</sub>O<sub>3</sub> hydrogenation type catalyst. The nonsulphided catalysts were activated by reduction ex situ. After reduction in H<sub>2</sub> atmosphere, the catalysts were stabilised using 1 vol% O<sub>2</sub> in N<sub>2</sub> for 5 h, in order to avoid reoxidation of the catalyst during loading into the BRS. The flowrate of different gases during activation was 225–250 mL/min.

### 10.2.2.6 Results: Hydrotreatment using a sulphided catalyst (second stage)

Continuous hydrotreatment of renewable Hydrofaction™ crude oil was successfully carried out on a sulphided NiMo/Al<sub>2</sub>O<sub>3</sub> catalyst. Two different campaigns were carried out with 380 and 660 h on stream, respectively. A standard renewable Hydrofaction™ crude oil with a sulphur content of 309 ppm was used in the first campaign (non-spiked). Based on observations indicating potential desulphurisation of the catalyst (Fig. 10.4), a similar renewable crude oil (oil B) was spiked to 1 wt% sulphur in the

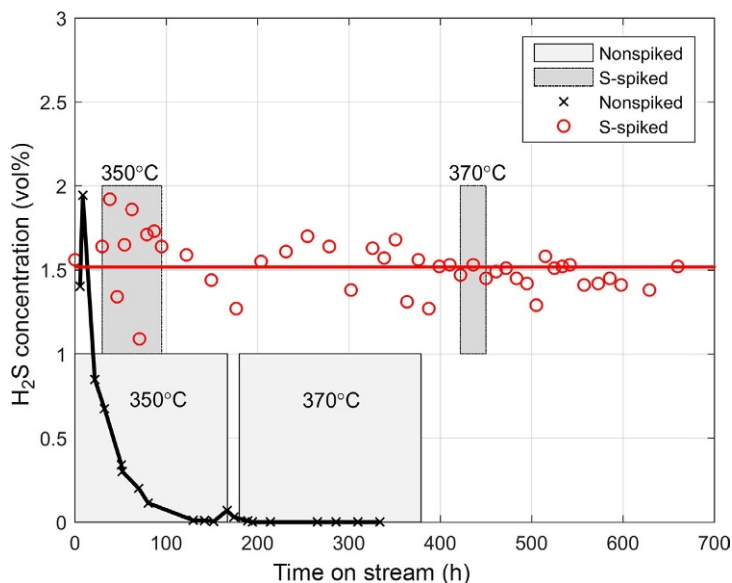


**Fig. 10.4**  $\text{H}_2\text{S}$  concentration of the product gas during the two continuous hydrotreating campaigns.

second campaign (spiked). Additionally, data from two different hydrotreating temperatures will be presented for each campaign, adding up to four different datasets. In the spiked campaign, several other operating parameters were screened, but these are left out of the current study for simplicity.

Table 10.3 lists the hydrotreating conditions of the different experiments, together with mass balance data and the product gas composition. At first sight, the datasets appear rather similar with mass balances closing to 93%–96% and with volumetric oil yields between 96 and 100 vol%. However, it is worth focusing on the gas composition and in particular the concentration of  $\text{H}_2\text{S}$ , which is also pictured as a function of time on stream for the two campaigns in Fig. 10.4. It is clear that the  $\text{H}_2\text{S}$  concentration is stable throughout the *s*-spiked campaign, whereas it drops to below detection level during the first 150 h on stream in the nonspiked campaign. This depicts the reasoning behind testing the effect of crude oil sulphur content.

Table 10.4 lists physiochemical properties of the renewable crude oils used as feedstock for the two campaigns and the corresponding hydrotreated products. Complete deoxygenation and TAN elimination were achieved at both temperatures applied during both campaigns. Furthermore, the viscosity is reduced almost three orders of magnitude. Density, HHV, and H/C ratios indicate that the hydrogenation is improved during the spiked campaign. This observation is supported by the hydrogen consumptions (Table 10.3), which seem slightly higher for the spiked campaign as compared with the nonspiked campaign. This is an important finding, since a high degree of hydrogenation is desirable when producing diesel and marine drop-in fuels. Likewise, it is clear from both campaigns that the higher operating temperature (370°C) reduces

**Table 10.3 Hydrotreating conditions, mass balance results, and product gas composition at two operating temperatures for both the nonspiked and sulphur-spiked upgrading campaign**

	Unit	Nonspiked		Spiked	
<i>Operational data</i>					
Flowrate	(mL/min)	0.30	0.30	0.33	0.33
Temperature	(C)	350	370	350	370
Pressure	(bar)	62	62	66	66
LHSV	(h <sup>-1</sup> )	0.5	0.5	0.5	0.5
H <sub>2</sub> availability	(NL/L)	900	900	900	900
Mass balance	(wt%)	93.5	93.3	94.0	95.6
Gas yield	(wt%)	5.5	6.7	4.3	5.0
H <sub>2</sub> consumption	(wt%)	1.9	1.9	2.4	2.2
Water content	(wt%)	9.4	9.1	6.7	7.7
Hydrocarbon yield	(wt%)	81.0	80.0	85.5	84.6
Hydrocarbon yield	(vol%)	99.7	98.2	97.4	96.0
<i>Gas composition</i>					
H <sub>2</sub>	(vol%)	94.6	93.0	96.1	93.9
H <sub>2</sub> S	(vol%)	0.3	0.0	1.6	1.5
C <sub>1</sub>	(vol%)	1.7	2.3	0.6	1.4
C <sub>2</sub>	(vol%)	0.5	0.9	0.2	0.4
C <sub>3</sub>	(vol%)	0.2	0.5	0.1	0.3
C <sub>4</sub>	(vol%)	1.2	1.1	0.7	1.1
C <sub>5</sub>	(vol%)	0.0	0.0	0.0	0.0
CO <sub>2</sub>	(vol%)	1.3	1.3	0.7	1.4
CO	(vol%)	0.1	0.9	0.0	0.0

**Table 10.4 Physiochemical properties of the products obtained at different conditions as compared with the renewable crude oils used as feedstock**

	Unit	Oil G	Nonspiked		Oil B <sup>c</sup>	Spiked	
Op. temperature	(C)	—	350	370	—	350	370
Density at 15°C	(kg/m <sup>3</sup> )	1103	989	989	1073	942	945
TAN	(mg/g)	55.7	<0.0	<0.0	48.0	<0.0	<0.0
Viscosity at 20°C	(cP)	80432	297	166	14429	34	33
HHV <sup>a</sup>	(MJ/kg)	37.2	42.1	42.2	38.0	43.3	43.2
Carbon <sup>a</sup>	(wt%)	80.6	88.1	88.4	80.4	88.6	87.4
Hydrogen <sup>a</sup>	(wt%)	9.1	11.9	11.6	9.0	13.4	12.6
Nitrogen <sup>a</sup>	(ppm)	1500	1175	986	822	424	402
Sulphur <sup>a</sup>	(ppm)	309	389	212	195	764	572
Oxygen <sup>b</sup>	(wt%)	10.1	0.0	0.0	10.4	0.0	0.0
H/C	(—)	1.34	1.61	1.57	1.34	1.84	1.71

<sup>a</sup> On dry basis.

<sup>b</sup> Oxygen by difference.

<sup>c</sup> Analysis before spiking with C<sub>4</sub>H<sub>10</sub>S.

hydrogenation as compared with 350°C. This is because hydrogenation is an exothermic reaction that is favoured by lower temperatures until reaction kinetics become rate limiting [22]. As a result, the continuous hydrotreating experiments suggest that the hydrogenation activity of the catalyst is reduced for a low-sulphur renewable crude oil compared with a sulphur-spiked equivalent.

HDN seems to be improved by both a higher operating temperature and a catalyst in its sulphided state (spiked campaign). Whereas the sulphur content is rather unchanged for products of the nonspiked campaign, it has increased in the products of the spiked campaign as compared with the biocrude. This is most likely due to H<sub>2</sub>S trapped in the products, because the hydrotreating setup did not enable stripping of H<sub>2</sub>S from the products.

Simulated distillation curves of the hydrotreated products are given in Fig. 10.5. True-boiling-point (TBP) distillation was also carried out and given in Fig. 10.5 of both the renewable crude oil and the 350°C samples from both the spiked and nonspiked campaigns.

The deoxygenation results in a significant degree of volatilisation and boiling-point reduction during hydrotreatment. In particular, products of the spiked campaign have been improved as compared with the simulated distillation of the renewable crude oil. The IBP-390°C distillate is improved with more than 30% in the spiked products compared with the renewable crude oil, whereas it is only around 10% for the nonspiked

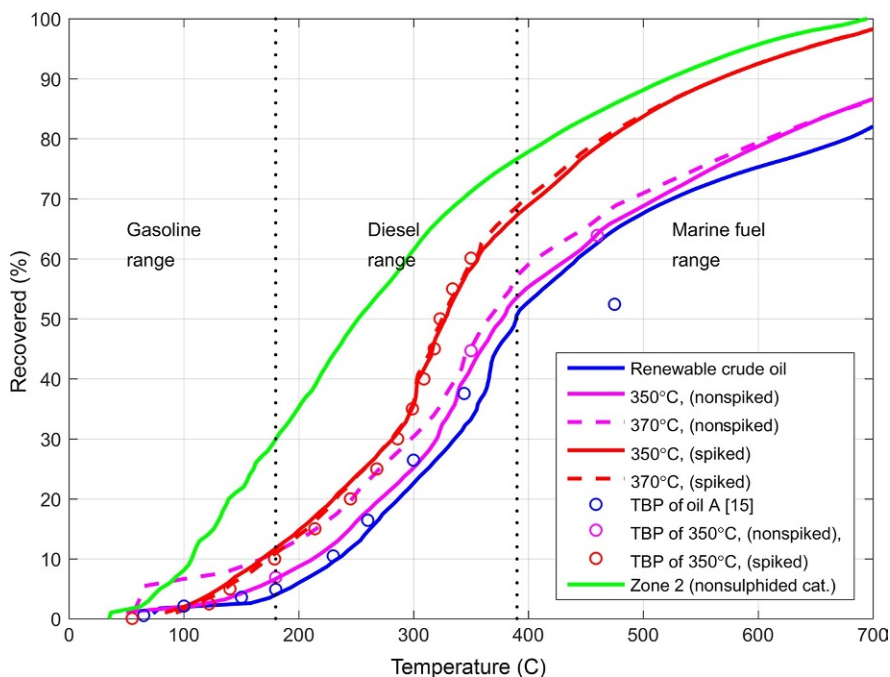


**Fig. 10.5** Simulated distillation (ASTM D7169) profiles of the hydrotreated products compared with the renewable crude oil. TBP refers to a true-boiling-point distillation (ASTM D2892).



products. This indicates that cracking of heavy ends is improved when the catalyst is kept in sulphided state by sulphur spiking. The operating temperature of a specific campaign seems to have less effect on the boiling-point distribution. A higher degree of cracking is observed at 370°C for both campaigns but at the cost of a reduced degree of hydrogenation.

### 10.2.2.7 Results: Two-zone upgrading using nonsulphided catalyst (second stage)

The use of nonsulphided hydrotreating catalysts for upgrading of a low-sulphur renewable Hydrofaction™ crude oil may prove beneficial, because expensive gas cleaning equipment may be avoided when H<sub>2</sub>S is reduced/avoided in the gaseous products. In Section 10.2.2.6, it was found that the hydrogenation and cracking activity of a sulphided catalyst is reduced when processing a low-sulphur renewable crude oil. Hydrogenation is however very important, when the objective is to produce diesel and marine fuel drop-in products. Based on a desire to improve the H/C ratio, a two-zone upgrading process was proposed, where deoxygenation and reduction of the boiling-point distribution is the objective of the first zone, while deep hydrogenation to improve the H/C ratio is the objective of the second zone. A schematic of such process is depicted in Fig. 10.6.

Initial screening of the nonsulphided catalysts was carried out to evaluate their ability to deoxygenate and hydrogenate the renewable crude oil. The screening included variation of temperature, pressure, and space velocity. The approach of the study was to initially screen the nonsulphided catalysts in microbatch reactors and

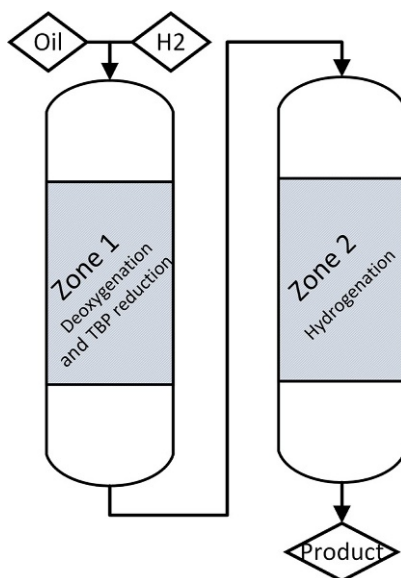


**Fig. 10.6** Schematic of two-zone upgrading approach that is tested using nonsulphided catalysts.

then batchwise upgrade enough oil at the optimum conditions of zone 1 and zone 2 to analyse both the intermediate zone 1 product and the final zone 2 product from such two-zone upgrading. An initial parameter screening resulted in a preferred set of operating conditions for each catalyst shown in Table 10.5. Multiple zone 1 experiments at these conditions were carried out to obtain sufficient oil to enable analysis and have enough feedstock for the zone 2 experiments that were also carried out a number of times to get enough samples for analyses.

The amount of sample from the BRS limits the amount of possible analyses, but density, HHV, and elemental composition are given in Table 10.6 for the renewable crude oil, the intermediate zone 1 product, and the final zone 2 product. The oxygen content is reduced to 0.7 wt% in zone 1 and further reduced to below detection level in zone 2. The hydrogenation facilitates an overall increase in H/C molar ratio from 1.25 to 1.58, which indicates a noticeable degree of dearomatisation. This is less than the H/C ratios achieved during the spiked campaign in the CRS (Table 10.4). However, the noble metal loading of the Pd catalyst was only around 500 ppm, and the H/C ratio is likely improved further by increasing the metal loading of this catalyst. The purpose of each reaction zone or catalyst is effectively visualised by the FTIR spectra given in Fig. 10.7. The spectra show that absorption from oxygenated functional groups in the Hydrofaction™ oil is nearly eliminated during the zone 1 reaction. Likewise, the olefinic and aromatic absorption are reduced during the zone 2 reaction, which indicates hydrogenation reactions.

Additional quality improvements are reflected by a 16% increase in HHV and a 15% reduction of the bulk density. Both the HHV and especially the density are improved

**Table 10.5 Preferred set of operating conditions based on the initial screening of the catalysts**

	Catalyst	Temperature	Pressure	WHSV*
Zone 1	NiW/SiO <sub>2</sub> /Al <sub>2</sub> O <sub>3</sub>	350°C	~100 bar	0.5 h <sup>-1</sup>
Zone 2	Pd/Al <sub>2</sub> O <sub>3</sub>	300°C	~100 bar	1.0 h <sup>-1</sup>

**Table 10.6 Product quality before, between, and after the two reaction zones using nonsulphided catalysts**

	Density <sup>a</sup> (kg/m <sup>3</sup> )	HHV <sup>b</sup> (MJ/kg)	Elemental comp. <sup>b</sup> (wt%)					H/C (-)
			C	H	N (ppm)	S (ppm)	O <sup>c</sup>	
Oil A [21]	1051	38.6	81.4	8.6	1124	100	9.8	1.26
Zone 1 product	914	42.4	89.0	10.3	66	61	0.7	1.38
Zone 2 product	892	43.5	88.3	11.7	<sup>d</sup>	<sup>d</sup>	0.0	1.58

<sup>a</sup> Density at 15°C.

<sup>b</sup> On dry basis.

<sup>c</sup> Oxygen by difference.

<sup>d</sup> Insufficient sample.

compared with the products obtained using sulphided catalysts (Table 10.4). Finally and perhaps most importantly, the simulated distillation profile of the zone 2 product (Fig. 10.5) shows a remarkable improvement of the amount of distillates compared with the products obtained using the sulphided catalyst. More specifically, the IBP-390°C distillate fraction increased by 50% compared with the renewable crude oil. As a result, the initial screening of a two-zone upgrading process with nonsulphided catalyst appears as a promising route for upgrading of Hydrofaction™ crude oil. Though, long term catalyst activity and stability need to be studied in a continuous reactor system.

### 10.3 Life cycle GHG emissions of Hydrofaction™

The sustainability of a renewable drop-in fuel is highly dependent on the energy efficiency of the production and the GHG emission reduction associated with use of the particular fuel. This section presents a calculation of the life-cycle GHG emission reductions associated with Hydrofaction™ products. The calculation is based on a 2000 barrel/day (BPD) Hydrofaction™ plant using forestry residues as feedstock and producing diesel and marine drop-in renewable fuels. Fig. 10.8 visualises the overall mass and energy flows for the 2000 BPD Hydrofaction™ plant assessed in the

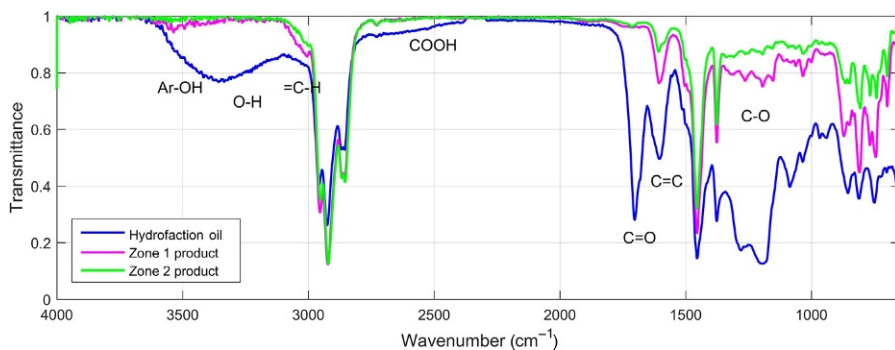


Fig. 10.7 Change in FTIR spectra during the two-zone upgrading process.

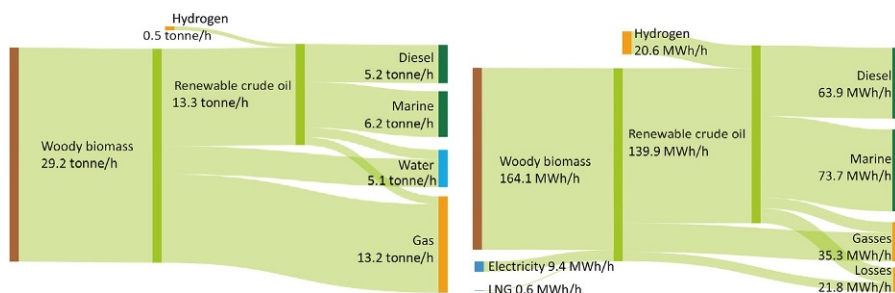


Fig. 10.8 Sankey diagrams of mass and energy balances in a potential 2000 BPD Hydrofaction™ plant.

GHG emission calculation. Mass and energy balances are based on the yield figures presented for the first and second Hydrofaction™ stage. More specifically, mass and energy balances for the first-stage Hydrofaction™ HTL are based on Ref. [21], while mass balances for the second stage are based on the *s*-spiked continuous upgrading experiment presented in Section 10.2.2.6. Fig. 10.8 illustrates the significant heating value that is available through the gaseous products from Hydrofaction™. In steady-state operation, combustion of these gaseous products is more than sufficient to make the overall process self-sustained with heat. However, an external LNG stream is included to cover start-up operations. Based on the energy balance in Fig. 10.8, the energy efficiency of the process can be calculated to 71%, which means that 71% of the energy added to the process is recovered in the drop-in fuels.

The location of the potential Hydrofaction™ plant assessed is the province of Alberta, Canada. Forestry residues are abundant in the region (Section 10.1.1), and fuel distribution infrastructure is widely available because extraction, refining, and distribution of oil sands and derived products is the largest industry in Alberta. Table 10.7 lists the emission intensities used in the GHG analysis of a Hydrofaction™ plant located in Alberta, Canada. Emission factors given in Ref. [15] by the government of Alberta have been used whenever possible. The plant applies forestry residues as feedstock that would have otherwise been disposed in permanent wood waste stockpiles. The methane emissions from decomposition of such wood waste stockpiles in the baseline scenario have been calculated based on the guidelines in Ref. [15]. It is assumed that the feedstock is transported on average 200 km from the harvesting site [16,35]. The gaseous Hydrofaction™ products are combusted to provide process heat, and the emission intensities of CH<sub>4</sub> and N<sub>2</sub>O combustion products are assumed equal to that from combustion of liquefied natural gas (LNG). LNG is purchased to cover any additional heat requirements related to process start-up. The effect of using standard grid electricity versus renewable grid electricity has been tested. Heat, electricity, and make-up HTL catalyst requirements are based on design studies for a 2000 BPD Hydrofaction™ plant. Upgrading catalysts is assumed to be changed once every year, and transportation of all make-up catalysts to site is assumed to be on average 1000 km by heavy truck. Hydrogen consumption during upgrading is defined to a conservative 4 wt% (oil feed basis), higher than shown in Fig. 10.8, in order to accommodate for improved hydrogenation and losses from process gas recirculation. The upgraded Hydrofaction™ oil is fractionated into 50 vol% renewable drop-in diesel fuel used to displace petroleum diesel and 50 vol% drop-in marine fuel used to displace heavy fuel oil. Emissions related to distribution and dispensing of the finished fuels are left out of the calculation, because it is assumed to be the same and independent of the carbon origin of the fuel. Finally, GHG emissions related to construction of the plant are assumed negligible over the lifetime of the plant.

Table 10.8 lists the GHG emissions related to a 2000 BPD Hydrofaction™ plant producing diesel and marine fuel as compared with a baseline scenario where petroleum-derived diesel and heavy fuel oil products are refined and used in Alberta, Canada. The GHG emission reduction associated with using Hydrofaction™ products as compared with petroleum-derived products is 77%. This is comparable with the 70% GHG emission reduction determined for hydrotreated HTL fuel by Ref. [5], where emissions related to plant construction are also neglected.

**Table 10.7 Emission intensities used in the GHG emission analysis of Hydrofaction™ products**

Emission source	Unit	CO <sub>2</sub>	CH <sub>4</sub>	N <sub>2</sub> O	CO <sub>2</sub> e <sup>a</sup>	Reference
Feedstock harvesting and transportation (200m), 15.9L diesel/tonne	(kg/tonne)	4.2E+01	2.1E-03	6.4E-03		[15,16,35]
Combustion of liquefied natural gas (LNG)	(kg/m <sup>3</sup> LNG)	1.9E+00	3.7E-04	3.3E-05		[15]
Emission factor for grid electricity	(kg/kWh)	BNA			6.4E-01	[15]
Emission factor for renewable grid electricity	(kg/kWh)	BNA			0.0E+00	
Hydrogen emission intensity	(kg/kg H <sub>2</sub> )	BNA			8.9E+00	[36]
K <sub>2</sub> CO <sub>3</sub> emission intensity	(kg/kg)	BNA			2.7E-01	[37]
NaOH emission intensity	(kg/kg)	BNA			4.7E-01	[38]
Upgrading catalyst emission intensity	(kg/kg)	BNA			5.5E+00	[39]
Catalyst transportation by truck, 1000 km	(kg/kg)	BNA			4.9E-02	[40]
Emission intensity of fuel extraction and production	(kg/L)	1.4E-01	1.1E-02	4.0E-06		[15]
Combustion of diesel	(kg/L)	2.7E+00	1.3E-04	4.0E-04		[15]
Combustion of heavy fuel oil	(kg/L)	3.1E+00	3.4E-05	6.4E-05		[15]
Emission intensity from decomposition of wood waste stockpile	(kg/tonne)	Biogenic	2.0E+01			[15]

<sup>a</sup> 1 kg CH<sub>4</sub> = 25 kg CO<sub>2</sub>e; 1 kg N<sub>2</sub>O = 298 kg CO<sub>2</sub>e; [15] BNA, breakdown not available.

**Table 10.8 GHG emission reduction associated with displacement of diesel and heavy fuel oil by renewable Hydrofaction™ products**

Emission source	Amount		CO <sub>2</sub> (kg/h)	CH <sub>4</sub> (kg/h)	N <sub>2</sub> O (kg/h)	CO <sub>2</sub> e* (kg/h)
<b>2000 BPD Hydrofaction™ plant</b>						
Feedstock collection and transport	29.2	tonne/h	1.2E+03	6.2E-02	1.9E-01	1295
Combustion of HTL process gas	3436	m <sup>3</sup> LNGe/h	Biogenic	1.3E+00	1.1E-01	66
Combustion of purchased LNG for heat	60.9	m <sup>3</sup> /h	1.2E+02	2.3E-02	2.0E-03	118
Purchased electricity	9362	kWh/h	BNA	BNA	BNA	5992
Purchased hydrogen	530	kg/h	BNA	BNA	BNA	4717
Drop-in diesel fuel usage	6.5	m <sup>3</sup> /h	Biogenic	8.6E-01	2.6E+00	791
Drop-in marine fuel usage	6.5	m <sup>3</sup> /h	Biogenic	2.2E-01	4.1E-01	129
Make-up catalysts	1087	kg/h	BNA	BNA	BNA	443
CO <sub>2</sub> sequestration	0	tonne/h	BNA	BNA	BNA	0
Hydrofaction™ GHG emission total						13550
<b>Petroleum baseline</b>						
Extraction and refining of petroleum diesel and fuel oil	12.9	m <sup>3</sup> /h	1.8E+03	1.4E+02	5.2E-02	5313
Diesel combustion	6.5	m <sup>3</sup> /h	1.7E+04	8.6E-01	2.6E+00	17974
Heavy fuel oil combustion	6.5	m <sup>3</sup> /h	2.0E+04	2.2E-01	4.1E-01	20287
Wood waste stockpiling, decomposition	29.2	tonne/h	Biogenic	5.9E+02		14642
Baseline GHG emission total						58216
GHG emission reduction						44666
GHG emission reduction relative to baseline						77

Table 10.8 lists the details of a base-case scenario where the Hydrofaction™ process purchases all the hydrogen required for upgrading and uses standard grid electricity (coal-intensive in Alberta) and where the biogenic CO<sub>2</sub> from the HTL gaseous products is all emitted. It is clear that the major contributions to GHG emissions from Hydrofaction™ are related to the purchased electricity and hydrogen, covering 44% and 35% of the total emissions, respectively. Based on that, the following three additional scenarios were tested in the LCA.

**Case 1:** The base case is modified so hydrogen produced in situ during first-stage Hydrofaction™ is applied during upgrading of the renewable crude oil to lower the amount of hydrogen that need to be purchased. No additional LNG needs to be purchased, because there is sufficient heating value in the remaining gaseous products after hydrogen separation. Additional electricity demand is not accounted for.

**Case 2:** The base case is modified so renewable grid electricity is used to reduce the emission intensity of electricity but at the expense of a higher cost.

**Case 3:** The base case is modified so all the biogenic CO<sub>2</sub> from the HTL gaseous products is extracted (before combusting the gaseous products with air) and sequestered. Additional electricity demand is not accounted for.

**Case 4:** The base case is modified to include all of the above.

Fig. 10.9 compares the GHG emissions from the different scenarios and the resulting emission reduction. The effect of utilising in situ produced hydrogen in case

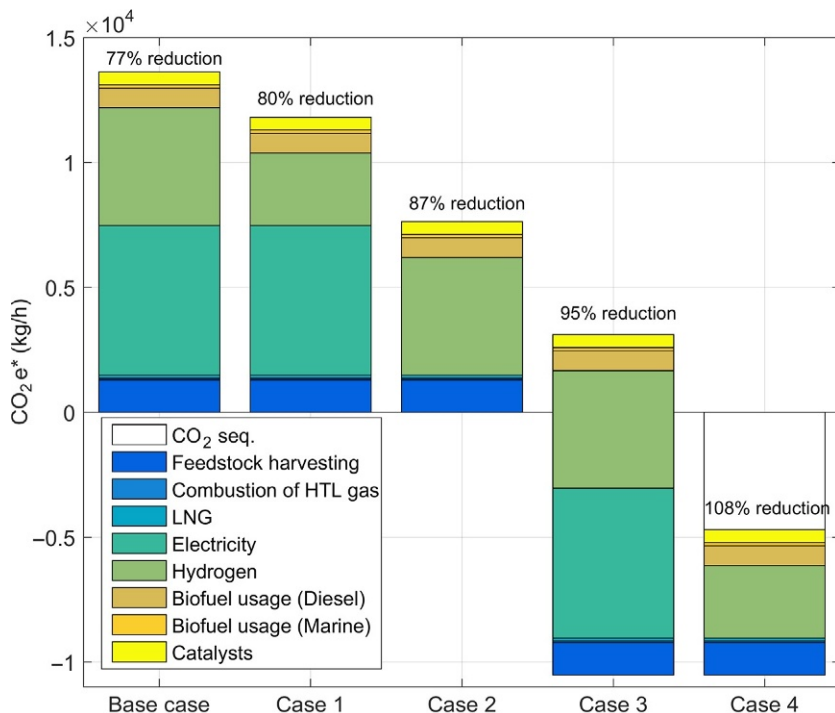


Fig. 10.9 GHG emission intensity of different Hydrofaction™ cases.

1 is minor, but this process modification is likely to be cost-efficient, since hydrogen is an expensive utility. The use of renewable electricity instead of standard grid electricity in case 2 has a major effect on the GHG emissions, which is because power generation in Alberta is relatively carbon-intensive due to coal-fired power plants. The cost-efficiency of case 2 depends on carbon legislation and the additional price of renewable electricity. The possibility of sequestering CO<sub>2</sub> from the HTL gaseous products is also worth considering as illustrated with case 3, since CO<sub>2</sub> is a major product from the first-stage Hydrofaction™ HTL and sequestration can significantly enhance the project's GHG emission savings. The rightmost column of Fig. 10.9 includes all the modifications to show the potential GHG emission reduction associated with Hydrofaction™ products. The result is a 108% GHG emission reduction, which implies a process that is not only CO<sub>2</sub> neutral but actually CO<sub>2</sub> negative.

## 10.4 Conclusion

Hydrofaction™ aims to fill the need for renewable heavy-transport fuels by converting forestry residues into drop-in renewable diesel and marine fuel using supercritical HTL and subsequent hydrotreating. Process descriptions and details are provided and supported by experimental data from continuous pilot operations. A comparison of six renewable Hydrofaction™ crude oils produced by supercritical HTL from different pine, spruce, birch, and bark mixtures shows similar quality independent of the woody feedstock. The characteristic fuel properties of these oils were significantly improved during two continuous hydrotreating campaigns with 300 and 700h on stream. The low sulphur content (100–200ppm S) of the crude oils was however found to inhibit the activity of the sulphided catalyst. A two-zone deoxygenation and hydrogenation reactor system using nonsulphided catalysts was screened in batch reactors, and improved devolatilisation relative to the sulphided catalysts was observed. Finally, mass and energy balances for a 2000 BPD Hydrofaction™ plant indicate that 1 tonne forestry residues can be converted to more than 400L renewable diesel and marine fuels with an energy recovery of 71% and a GHG emission reduction of 77%–108%, reflecting an energy- and resource-efficient technology for the production of renewable fuels for heavy transportation.

## Acknowledgements

The authors are thankful for the collaboration with Professor Lasse A. Rosendahl, Aalborg University, Denmark, and Professor Pedro Pereira Almao and his team at University of Calgary, Canada. The authors acknowledge the funding provided by EASME Horizon 2020 (Grant No. 666712), Danish Energy Technology Development and Demonstration Program (Grant No. 64013-0513), and Innovation Fund Denmark (Grant No. 4135-00126B).



## References

- [1] IPCC (2014), *Climate Change 2014: Synthesis Report. Contribution of Working Groups I, II and III to the Fifth Assessment Report of the Intergovernmental Panel on Climate Change*, (Core Writing Team: R.K. Pachauri and L.A. Meyer (eds.)). IPCC, Geneva, 151 pp.
- [2] United Nations/Framework Convention on Climate Change (2015) Adoption of the Paris Agreement, 21st Conference of the Parties, Paris, France, United Nations.
- [3] IEA (2016), *World energy outlook 2016, Executive summary*, Tech. rep., International Energy Agency. Paris.
- [4] [European Commission. Communication from the commission to the european parliament, the council, the european economic and social committee and the committee of the regions. A european strategy for low-emission mobility; 2016. SWD\(2016\), 244 final, Brussels, Belgium.](#)
- [5] I. Tews, Y. Zhu, C. Drennan, D. Elliott, L. Snowden-Swan, K. Onarheim, Y. Solantausta, D. Beckman (2014), *Biomass direct liquefaction options: Technoeconomic and life cycle assessment*, Tech. Rep., Prepared for U.S. Department of Energy, Springfield.
- [6] [De Jong S, Faaij A, Slade R, Mawhood R, Junginger M. The feasibility of short-term production strategies for renewable jet fuels is—a comprehensive techno-economic comparison. \*Biofuels Bioprod Biorefin\* 2015;9\(6\):778–800.](#)
- [7] [Jensen CU, Hoffmann J, Rosendahl LA. Co-processing potential of HTL bio-crude at petroleum refineries. Part 2: A parametric hydrotreating study. \*Fuel\* 2016;165:536–43.](#)
- [8] FAO (2016), *State of the World's Forests 2016. Forests and Agriculture: Land-Use Challenges and Opportunities*. Food and Agriculture Organization of the United Nations, Rome.
- [9] [Ramachandran Nair PK, Mohan KB, Nair VD. Agroforestry as a strategy for carbon sequestration. \*J Plant Nutr Soil Sci\* 2009;172\(1\):10–23.](#)
- [10] [Millar CI, Stephenson NL, Stephens SL. Climate change and forests of the future: managing in the face of uncertainty. \*Ecol Appl\* 2007;17\(8\):2145–51.](#)
- [11] O'Laughlin, Jay, and Mahoney, Ron (2008), *Forests and Carbon*. From University of Idaho Extension's 'Woodland notes', 19, 2.
- [12] Bradley, D. (2007), *Canada- Sustainable forest biomass supply chains*. Prepared for IEA Task 40 by Climate change solution. Ottawa, Canada.
- [13] [Peter B, Niquidet K. Estimates of residual fibre supply and the impacts of new bioenergy capacity from a forest sector transportation model of the Canadian Prairie Provinces. \*Forest Policy Econ\* 2016;69:62–72.](#)
- [14] U.S. Department of Energy (2016), *2016 Billion-Ton Report: Advancing Domestic Resources for a Thriving Bioeconomy, Volume 1: Economic availability of feedstocks*. M. H. Langholtz, B. J. Stokes, and L. M. Eaton (Leads), ORNL/TM-2016/160. Oak Ridge National Laboratory, Oak Ridge, TN. 448p.
- [15] Government of Alberta (2015), *Carbon offset emission factors handbook, ESRD Climate Change 2015, No. 1, Alberta Carbon Offset Program*. Edmonton, Canada.
- [16] [Cambero C, Alexandre MH, Sowlati T. Life cycle greenhouse gas analysis of bioenergy generation alternatives using forest and wood residues in remote locations: a case study in British Columbia, Canada. \*Resour Conserv Recycl\* 2015;105:59–72.](#)
- [17] BTG BV (2002), *Methane and nitrous oxide emissions from biomass waste stockpiles*. Technical Report no. 12, Prepared for Worldbank PCFplus Research by Biomass Technology Group BV, Washington, DC.

- [18] Macdonald C. Market pulp:overcapacity on the way. *Pulp & Paper-Canada* 2016; 117(3):9–11.
- [19] RISI. China, Brazil paper and pulp production advances, even as growth slows globally, <http://www.risiinfo.com/press-release/china-brazil-paper-pulp-production-advances-even-growth-slows-globally/>; 2017. Accessed January 24, 2017.
- [20] FAO (2009), State of the World's Forests 2009. Food and Agriculture Organization of the United Nations, Rome, Italy.
- [21] Jensen CU, Guerrero JKR, Karatzos S, Olofsson G, Iversen SB. Fundamentals of Hydrofaction™: renewable crude oil from woody biomass. *Biomass Convers Biorefin* 2017; <https://doi.org/10.1007/s13399-017-0248-8>.
- [22] Gary JH, Handwerk GE, Kaiser MJ. Petroleum refining, technology and economics. 5th ed. CRC Press; 2007, ISBN: 0-8493-7038-8.
- [23] Lane, J. (2015), 4 minutes with... Taner Onoglu, Vice President, Altaca Energy. *Biofuels Digest*. <http://www.biofuelsdigest.com/bdigest/2015/06/04/4-minutes-with-taner-onoglu-vice-president-altaca-energy/>. [Accessed 21 February 2017].
- [24] Genifuel 2015. Genifuel corporation closeout report for NAABB program, DE-FOA-0000123 [http://www.energy.gov/sites/prod/files/2016/01/f28/naabb\\_genifuel\\_pilot\\_system\\_final\\_report.pdf](http://www.energy.gov/sites/prod/files/2016/01/f28/naabb_genifuel_pilot_system_final_report.pdf). [Accessed 21 February 2017].
- [25] Muradel Pty Ltd. (2017), Technology <http://www.muradel.com/aboutus.asp#tech>. [Accessed 21 February 2017].
- [26] Licella Pty Ltd. Cat-HTR, <http://www.licella.com.au/cat-htr/>; 2017.
- [27] Elliott DC, Biller P, Ross AB, Schmidt AJ, Jones SB. Hydrothermal liquefaction of biomass: developments from batch to continuous process. *Bioresour Technol* 2015;178:147–56.
- [28] Elliott DC. In: Process development for biomass liquefaction. Volume 25:4, Conference 180, Report no. CONF-800814-P3, Pacific Northwest Lab., American Chemical Society, Division of Fuel Chemistry, Richland, USA; 1980.
- [29] Harvey AH, Peskin AP, Klein SA. NIST/ASME Steam properties database, Software Version 3.0. In: Standard Reference Database. National Institute of Standards and Technology (NIST), US Department of Commerce; 2013.
- [30] Akiya N, Savage PE. Roles of water for chemical reactions in high-temperature water. *Chem Rev* 2002;102:2725–50.
- [31] Kruse A, Dinjus E. Hot compressed water as reaction medium and reactant properties and synthesis reactions. *J Supercritical Fluid* 2007;39:362–80.
- [32] Sintamarean IM, Grigoras IF, Jensen CU, Toor SS, Pedersen TH, Rosendahl LA. Two-stage alkaline hydrothermal liquefaction of wood to biocrude in a continuous bench scale system. *Biomass Convers Biorefin* 2017; <https://doi.org/10.1007/s13399-017-0247-9>.
- [33] Jensen CU, Olofsson G, Rosendahl LA. Impact of Nitrogenous Alkaline Agent on Continuous HTL of Lignocellulosic Biomass and Biocrude Upgrading. *Fuel Process Technol* 2017;159:376–85.
- [34] Hoffmann J, Jensen CU, Rosendahl LA. Co-processing potential of HTL bio-crude at petroleum refineries. Part 1: Fractional distillation and characterization. *Fuel* 2016;165:526–35.
- [35] McKechnie J, Chen J, Vakalis D, MacLean H. Energy use and greenhouse gas inventory model for harvested wood product manufacture in Ontario; 2014. Climate change research report, CCRR-39, Ontario, Canada.
- [36] Ruether J, Ramezan M, Grol E. Life-cycle analysis of greenhouse gas emissions for hydrogen fuel production in the United States from LNG and coal. *DOE/NETL-2006/1227*; 2005.

- 
- [37] Pendolovska, V., Fernandez, R., Mandl, N., Gugele, B., and Ritter, M. (2014), Annual European Union Greenhouse Gas Inventory 1990–2012 and Inventory Report 2014. Technical report no. 09/2014 by European Environment Agency. Copenhagen.
- [38] Biograce. Harmonised calculations of biofuel greenhouse gas emissions in Europe, list of standard values, <http://www.biograce.net/content/ghgcalculationtools/standardvalues>; 2017.
- [39] Snowden-Swan LJ, Spies KA, Lee GJ, Zhu Y. Life cycle greenhouse gas emissions analysis of catalysts for hydrotreating of fast pyrolysis bio-oil. *Biomass Bioenergy* 2016;86:136–45.
- [40] Railway association of Canada. Rail Freight Greenhouse Gas Calculator, <http://www.railcan.ca/environment/calculator>; 2017.